"In presenting the dissertation as a partial fulfillment of the requirements for an advanced degree from the Georgia Institute of Technology, I agree that the Library of the Institution shall make it available for inspection and circulation in accordance with its regulations governing materials of this type. I agree that permission to copy from, or to publish from, this dissertation may be granted by the professor under whose direction it was written, or, in his absence, by the dean of the Graduate Division when such copying or publication is solely for scholarly purposes and does not involve potential financial gain. It is understood that any copying from, or publication of, this dissertation which involves potential financial gain will not be allowed without written permission.

SHAPING MICROWAVE ANTENNA RADIATION PATTERNS BY AN APERTURE-FIELD METHOD

A THESIS

Presented to

the Faculty of the Graduate Division

By

Roland Eugene Moseley

In Partial Fulfillment

of the Requirements for the Degree

Master of Science in Electrical Engineering

Georgia Institute of Technology

June 1959

SHAPING MICROWAVE ANTENNA RADIATION PATTERNS

BY AN APERTURE-FIELD METHOD

Approved:

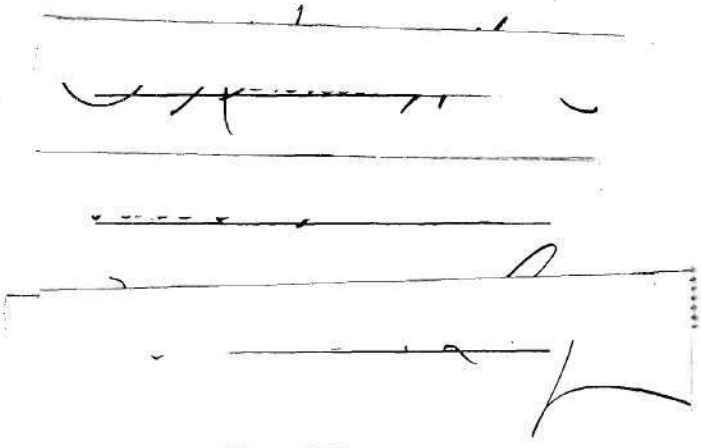

Date Approved by Chairman: May 20, 1959

ACKNOWLEDGEMENTS

The work herein described was partially supported by the U. S. Army Signal Research and Development Laboratory, Fort Monmouth, New Jersey, under Contract DA 36-039 SC-74870. It was made possible by use of the facilities of the Engineering Experiment Station of the Georgia Institute of Technology. The contribution to the work by members of the staff of the Radar Branch of the Engineering Experiment Station and by my thesis advisor, Dr. F. Kenneth Hurd, are gratefully acknowledged. A special note of appreciation is due my wife, Marita, for her patience and understanding.

TABLE OF CONTENTS

TABLE OF CONTENTS (Continued)

LIST OF ILLUSTRATIONS

SUMMARY

The purpose of this investigation was to demonstrate the applicability of analog computer techniques to the solution of microwave antenna beam-shaping problems. A description and an analysis of a method for obtaining a microwave reflecting surface for the purpose of achieving a desired antenna beam shape is given. This method utilizes an analog computer as a tool for completing a key step in the process.

Far-field radiation patterns of microwave antennas are described by an integral of the form

$$\overline{A(\theta)} = \int_{-a}^{a} \overline{f(y)} e^{j\frac{2\pi}{\lambda} \sin\theta \cos\theta\, dy} + \int_{-a}^{a} \overline{f(y)} e^{j\frac{2\pi}{\lambda} \sin\theta \cos\gamma\, dy};$$

for antennas where beam-shaping is restricted to narrow angular regions this may be further simplified to an integral of the form

$$\overline{A(\theta)} = \int_{-a}^{a} \overline{f(y)} e^{j\frac{2\pi}{\lambda} \sin\theta\, dy}.$$

Analog computers which will solve these integral equations are described. The computer which will solve the more general relation has not been constructed. The computer which will solve the narrow beam approximation is in existence at the Engineering Experiment Station of the Georgia Institute of Technology and it was used to demonstrate the applicability of the method. The function $\overline{f(y)}$ describes the distribution of energy (amplitude and phase) in the antenna aperture. When fed $\overline{f(y)}$ as data, these computers will calculate the far-field radiation pattern $A(\theta)$.

For a given beam-shaping problem the amplitude of the aperture energy distribution and the desired far-field radiation pattern are known. The known amplitude function and a series of trial phase functions are fed into the computer as data. The required phase function is then taken as the one which yields an acceptable far-field pattern. The required microwave reflecting surface is found from the phase function by utilizing a geometrical optics approximation.

The existing computer is employed in the solution of a problem consisting of the design and construction of a shaped-beam antenna which is a section of a parabolic cylinder with a beam-shaping surface attached at its lower extremity. Excellent correlation was obtained between the desired beam shape and the experimentally measured beam shape. In addition, a deviation of no more than 0.04 per cent of the peak intensity was observed over the beam shaping region between the calculated and experimental radiation patterns for this antenna.

CHAPTER I

INTRODUCTION

The Problem.--In practical microwave antenna problems, it is often desirable to shape the far-field radiation pattern to accomplish specific objectives. Herein is described a novel technique for obtaining a microwave reflecting surface, based on an aperture-field method (1)*, which will yield a far-field pattern of predicted shape when used in conjunction with the proper primary feed. This method is readily applicable to modifying parabolic cylinder reflectors; it can also be used for modifying paraboloids of revolution such as barrel- and shovel-reflectors. This method is based on the approximation that any planar aperture can be analyzed in terms of a succession of equivalent slit apertures.

History.--The highly directive beams attainable with microwave antennas are utilized to achieve a large antenna gain and a high degree of angular target resolution. The exploration of wide angular regions with such sharp beams requires a complex scanning operation in which scan time becomes a limiting factor. This problem is greatly simplified if the required scanning is limited to only one plane; then the coverage of the required angular region can be accomplished by merely "fanning" the beam. Thus scanning could be achieved by the use of a simple fan beam; however, this would usually result in a waste of power and unequal illumi-

---

*Numbers in parenthesis refer to the bibliography.

nation of targets located in different angular directions. To overcome these limitations it is necessary to impose on the beam, by special design techniques, some shape not characteristic of the normal diffraction lobe. The beam shape most often required is one that will illuminate identical targets located at various ranges in the same azimuth plane so that their received echo signals will be of equal magnitude. A $\csc^2 \theta$ distribution of power in the far-field will accomplish this (2), where θ is the angle between a normal to the aperture and the far-field direction in question.

Numerous methods have been employed in attempting to produce a beam which is flared asymmetrically in either the E- or H-plane and which has pencil beam characteristics in the transverse plane. Most of these are rather crude cut-and-try techniques; only one, which is a technique for modifying parabolic cylinder reflectors* described by L. J. Chu (4), is comparable with the method which is being described here. Chu's method is based on the energy-balance principle of geometrical optics and mathematically specifies the manner in which the reflector must be curved in order that the energy incident on each element of surface is reflected in the desired direction. The essential requirement of this technique is that there should be a one-to-one correspondence between each point on the aperture and each direction in the far-field radiation pattern. If this requirement is fulfilled, the power fed into a certain length of aperture can be equated tc the power radiated into a certain far-field angular range.

---

*Extended to doubly-curved surfaces by Silver (see reference number 3).

The Method.--It is shown in Chapter II that the far-field radiation pattern, $\overline{A(\theta)}$*, of a microwave antenna can be expressed in terms of (a) its aperture energy distribution function $\overline{f(y)}$, (b) the angle θ between a normal to the aperture and the far-field point in question, and (c) the angle γ between a normal to the aperture and the direction of energy flow at each point on the aperture. Thus $\overline{A(\theta)}$ is given by

$$\overline{A(\theta)} = \int_{-a}^{a} \overline{f(y)} e^{j\frac{2\pi}{\lambda} \sin\theta \cos\theta \, dy} + \int_{-a}^{a} \overline{f(y)} e^{j\frac{2\pi}{\lambda} \sin\theta \cos\gamma \, dy}. \quad (1)$$

Chapter II also shows that, for antennas where beam-shaping is restricted to narrow angular regions, Equation 1 can be further simplified to

$$\overline{A(\theta)} = 2\int_{-a}^{a} \overline{f(y)} e^{j\frac{2\pi}{\lambda} \sin\theta \, dy}. \quad (2)$$

Analog techniques which may be used to solve Equation 1 are discussed in Chapter III. In addition an existing analog computer, which will solve the narrow beam approximation (Equation 2), is described.

In Chapter IV the method of solution which is particular to this dissertation is described. It is seen that the operation of the method is facilitated by the use of analog computer techniques, such as those described in Chapter III, for solving Equations 1 and 2. A desired radiation pattern $A(\theta)$, having been assumed, analog techniques are then used to find the aperture energy distribution function, $\overline{f(y)}$, by employing a converging cut-and-try method. The required reflecting sur-

---

*The superscribed bar will be employed to designate a complex quantity.

face is then found from the aperture phase function utilizing the Elliptic Intersection Method (5), which involves a geometrical-optics approximation.

Experimental verification of the method is given in Chapter V where the ideal, predicted, and experimental radiation patterns for one specific problem are compared.

Comparison with Chu's Method.--Chu's method has one great weakness in that it ignores diffraction effects and hence gives no fine pattern detail. This is a deficiency which is inherent in any method based entirely on geometrical optics. Chu suggests that one should calculate the scattered field from the antenna, using the current-distribution method, to ascertain that diffraction effects do not render a solution useless. This is a long and tedious process which must be accomplished practically with digital computer equipment.

It is here that the present method is superior; the amplitude and phase of the aperture illumination function can be put into an analog antenna computer as data. The far-field pattern can then be determined automatically by the computer and recorded (in decibels) on an antenna pattern recorder. Detailed patterns can thus be obtained, subsequent to the alignment of the computer, in approximately 15 minutes.

CHAPTER II

DERIVATION OF RELATIONS BETWEEN APERTURE-FIELD AND FAR-FIELD

Derivation of the General Relation.--The electromagnetic field due to diffraction through a large planar aperture of arbitrary shape is described (6) by the scalar equation

$$\bar{A} = \frac{1}{4\pi} \int_S F(x,y) e^{j\psi(x,y)} \frac{e^{-jkr}}{r} \left[\left(jk + \frac{1}{r} \right) \vec{i}_z \cdot \vec{r} + jk\vec{i}_z \cdot \vec{s} \right] dS, \qquad (3)$$

where:

$\bar{A}$ is the scalar diffraction field at any point P of the right hemisphere.

$F(x,y)$ is the amplitude distribution of the field over the aperture S.

$\psi(x,y)$ is the phase of the field over the aperture.

k is $\frac{2\pi}{\lambda}$.

λ is the wavelength of the radiated energy.

$\vec{r}$, $\vec{i}_z$, $\vec{R}$, and $\vec{s}$ are unit vectors, the direction of $\vec{s}$ being the direction of power flow at a point x, y of the aperture; directions of the remaining vectors are given in Figure 1.

If P is sufficiently far from the aperture (in the far-field), the following simplifying assumptions can be made:

1. The distance r, except in the phase term e^{-jkr}, can be replaced by R, the distance from the field point to the origin.

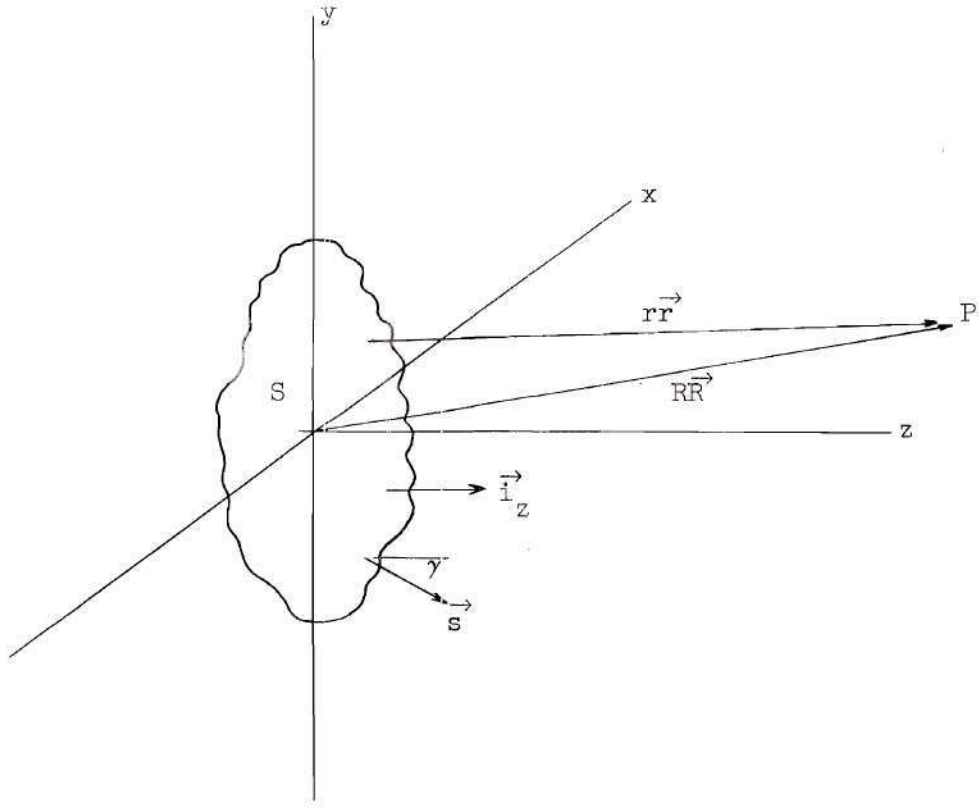

Figure 1. Aperture and Diffraction-Field Geometry

2. The term $\frac{1}{r}$ can be neglected in comparison with jk.

3. The directions of $\vec{r}$ and $\vec{R}$ with respect to the z-axis can be considered equal, permitting $\vec{i}_z \cdot \vec{r}$ to be replaced by $\vec{i}_z \cdot \vec{R} = \cos\theta$.

Equation 3 then becomes

$$\overline{A} = \frac{j}{2\lambda R} \int_S F(x,y) e^{j\Psi(x,y)} \, e^{-jkr} \left[\cos\theta + \cos\gamma\right] dS. \tag{4}$$

It is shown in the following paragraphs that if the energy along all of the line elements parallel to the x-axis and dy in width (see Figure 2) is summed with proper phase and amplitude and their resultant placed along the y-axis, then the far-field distribution of energy in the yz-plane is identical to that produced by the original aperture.

If P is constrained to move in the yz-plane in a circular path of large radius about the origin, the distances to P from all elements of the aperture with identical y-coordinates are equal, as can be seen from Figure 2. This distance is given by

$$r = R - y \sin\theta. \tag{5}$$

Substitution of this into Equation 4 gives

$$\overline{A} = \frac{j}{2\lambda R} e^{-jkR} \int_{y_1}^{y_2} e^{jky \sin\theta} \left[\int_{x_1(y)}^{x_2(y)} \overline{F(x,y)} \, dx \right] \times \left[\cos\theta + \cos\gamma\right] dy. \tag{6}$$

This may be rewritten as

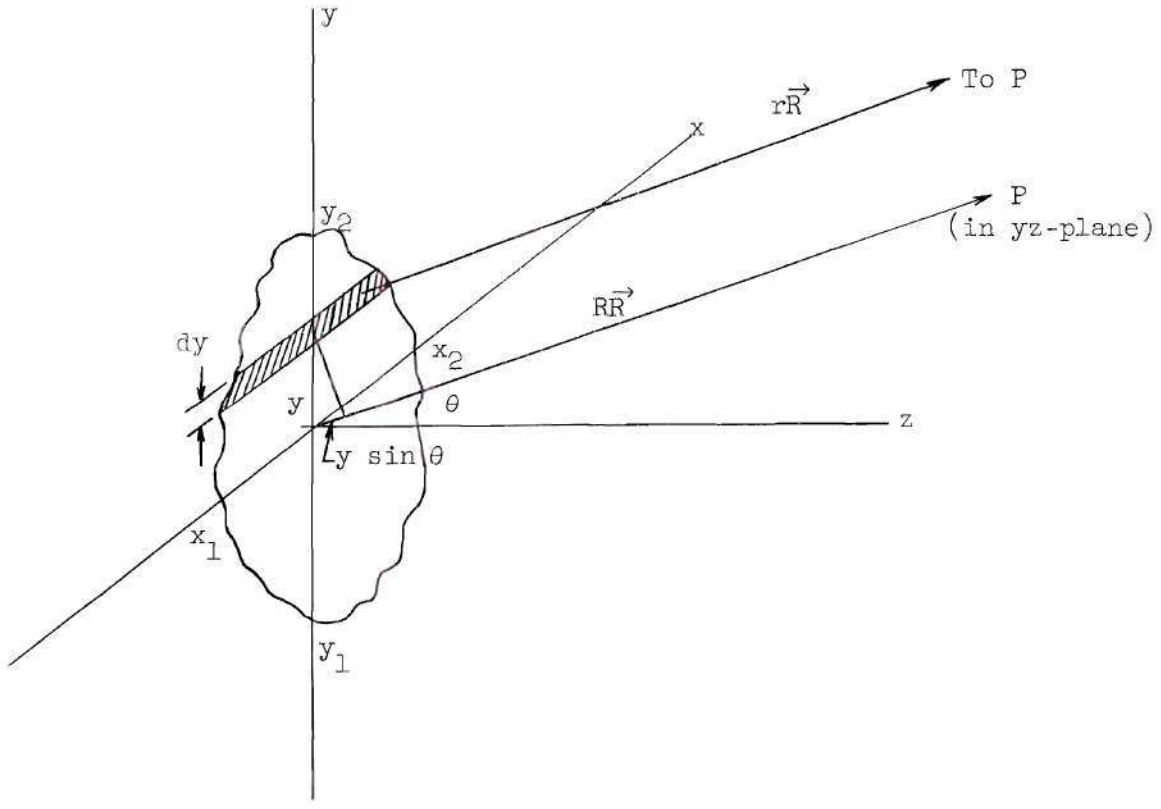

Figure 2. Aperture and Far-Zone Diffraction-Field Geometry

$$\overline{A} = \frac{j}{2\lambda R} e^{-jkR} \left[\int_{y_1}^{y_2} e^{jky \sin\theta} \left\{ \int_{x_1(y)}^{x_2(y)} \overline{F(x,y)}\, dx \right\} \cos\theta\, dy \right.$$

$$\left. + \int_{y_1}^{y_2} e^{jky \sin\theta} \left\{ \int_{x_1(y)}^{x_2(y)} \overline{F(x,y)}\, dx \right\} \cos\gamma\, dy \right] \quad (7)$$

where x_1, x_2, y_1, and y_2 are the x and y limits of the aperture and where $\overline{F(x,y)} = F(x,y)e^{j\psi(x,y)}$.

If the origin is located at the center of the aperture in the y-direction, Equation 7 can be written

$$\overline{A(u)} = \int_{-a}^{a} \overline{f(y)}\, e^{juy} \cos\theta\, dy + \int_{-a}^{a} \overline{f(y)}\, e^{juy} \cos\gamma\, dy \quad (8)$$

where

$$\overline{f(y)} = \int_{x_1(y)}^{x_2(y)} \overline{F(x,y)}\, dx \quad (9)$$

and where

u is k sin θ,

a is the half length of the aperture, and

A(u) is normalized.

Dropping the constant phase term e^{-jkR} is equivalent to rotation of the phase reference through the angle -kR.

By the above procedure, any planar aperture for which Equation 4 holds can be reduced to an equivalent slit aperture for exploration of the far-zone radiation field in a plane which contains the slit and the z-axis with the aperture oriented as in Figure 2. The complete radiation pattern can be determined from a succession of such slits, obtained by progressively rotating the x- and y-axis about the z-axis while holding the aperture fixed.

The Narrow Beam Approximation.--For a given aperture the narrowest possible beamwidth is obtained when the energy distribution over the aperture is constant in both amplitude and phase (7). Thus if the beam-shaping is confined to a narrow angular region near the z-axis, the phase over the aperture, $\psi(x,y)$, does not vary greatly and the terms $\cos\theta$ and $\cos\gamma$ in Equation 8 can be replaced by unity. Equation 8 then becomes

$$\overline{A(u)} = 2 \int_{-a}^{a} \overline{f(y)}\, e^{juy}\, dy. \qquad (10)$$

Discussion of Approximations and Limitations.--The approximations contained in the derivation of Equation 8 are the common far-field approximations and negligible error is incurred (8) as a result of them. Equation 8 is general and applicable to beam-shaping over wide angular regions. Discussed here are the approximations in going from the general relation (Equation 8) to the narrow beam approximation (Equation 10).

The $\cos\theta$ term, contained in the first integral of Equation 8, is an obliquity factor and it accounts for the apparent fore-shortening of

the aperture when it is viewed from wide angles. This term merely reduces $|\overline{f(y)}|$ for calculation of far-field points other than in the $\theta = 0$ direction. In the second integral of Equation 8 the direction of energy flow along the aperture is accounted for by the cos γ term, it is equal to its maximum value of 1 at all aperture points except those which contribute to beam-shaping; $|\overline{f(y)}|$ is reduced in these regions by cos γ.

There is no sharp dividing line which separates problems in which Equation 10 may be used from those in which Equation 8 must be used. Each problem must be examined on its own merit realizing that, in the transitional region, the allowable deviation from the desired beam-shape is the greatest single controlling factor in the application of these equations. Results have indicated that the shape of the far-field pattern is relatively insensitive to small variations in the aperture amplitude function, and that Equation 10 may usually be used if beam-shaping is confined to angles not greater than 30°.

CHAPTER III

ANALOG TECHNIQUES

It has been shown (9) that analog computer techniques are especially applicable to the solution of microwave antenna design problems. A description of a possible computer for the solution of the general relation between the aperture-field and the far-field is given. An existing computer (10) which solves the narrow beam aperture-field, far-field approximation is also described.

A Possible Computer for the General Relation.--This computer would determine the absolute value, $A(u)$, of the integral

$$\overline{A(u)} = \int_{-a}^{a} \overline{f(y)} e^{juy} \cos\theta \, dy + \int_{-a}^{a} \overline{f(y)} e^{juy} \cos\gamma \, dy. \qquad (11)$$

The factors of Equation 11 are simulated in the computer by electrical or mechanical analogs to obtain voltages which are proportional to $A(u)$. Since $A(u)$ can vary over wide limits in practical problems, the solution is recorded in decibels below the maximum value of $A(u)$. Values for $A(u)$ are obtained at discrete values of u which are spaced at small enough intervals that the solution does not vary greatly between successive computed values. Therefore, the envelope of the computed values closely approximates the required solution. A block diagram of the proposed computer is shown in Figure 3. This computer evaluates the integrals of Equation 11 sequentially; the timing diagram shown in Figure 4 indicates the sequence of events which take place during the evaluation

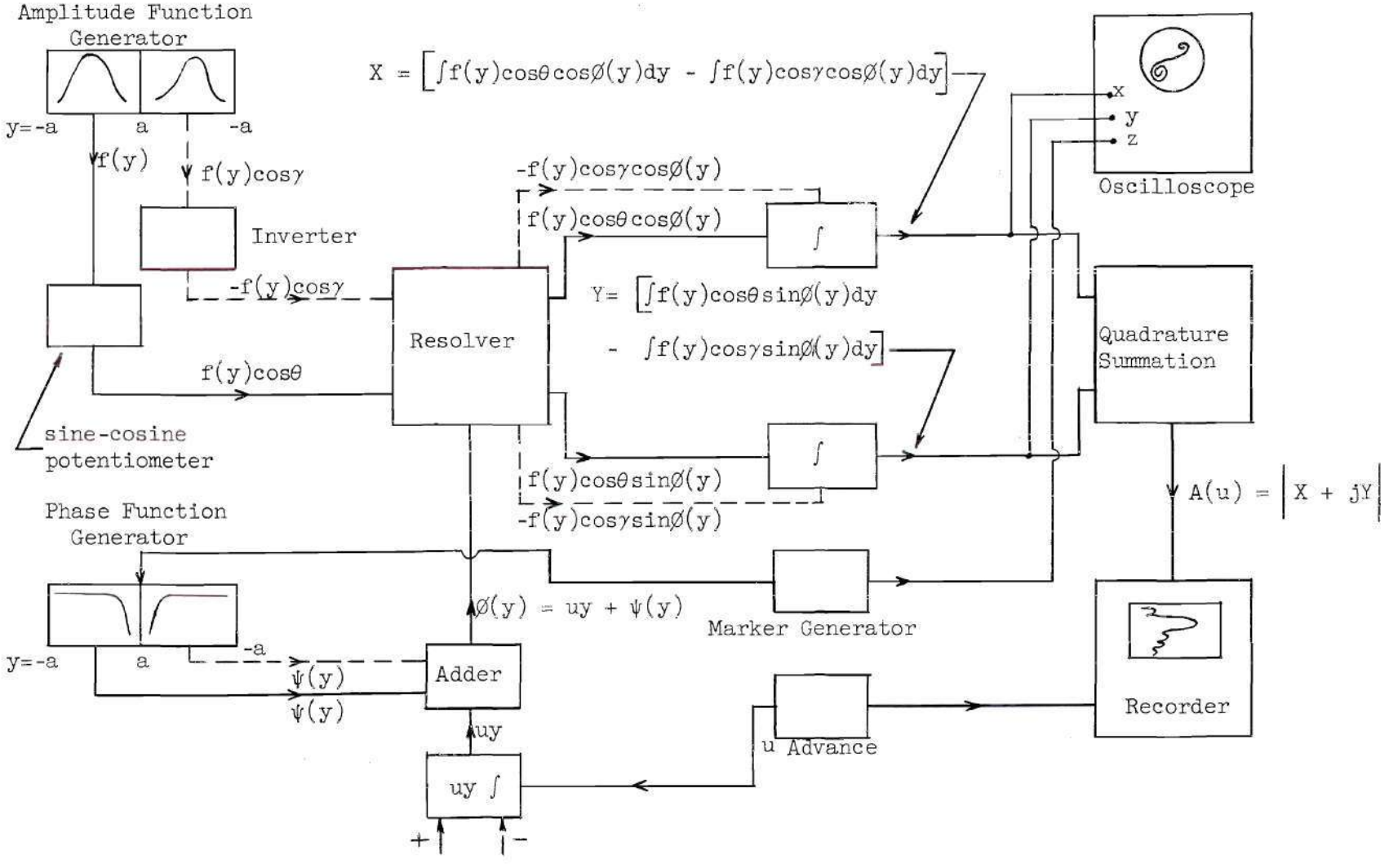

Figure 3. Proposed Computer

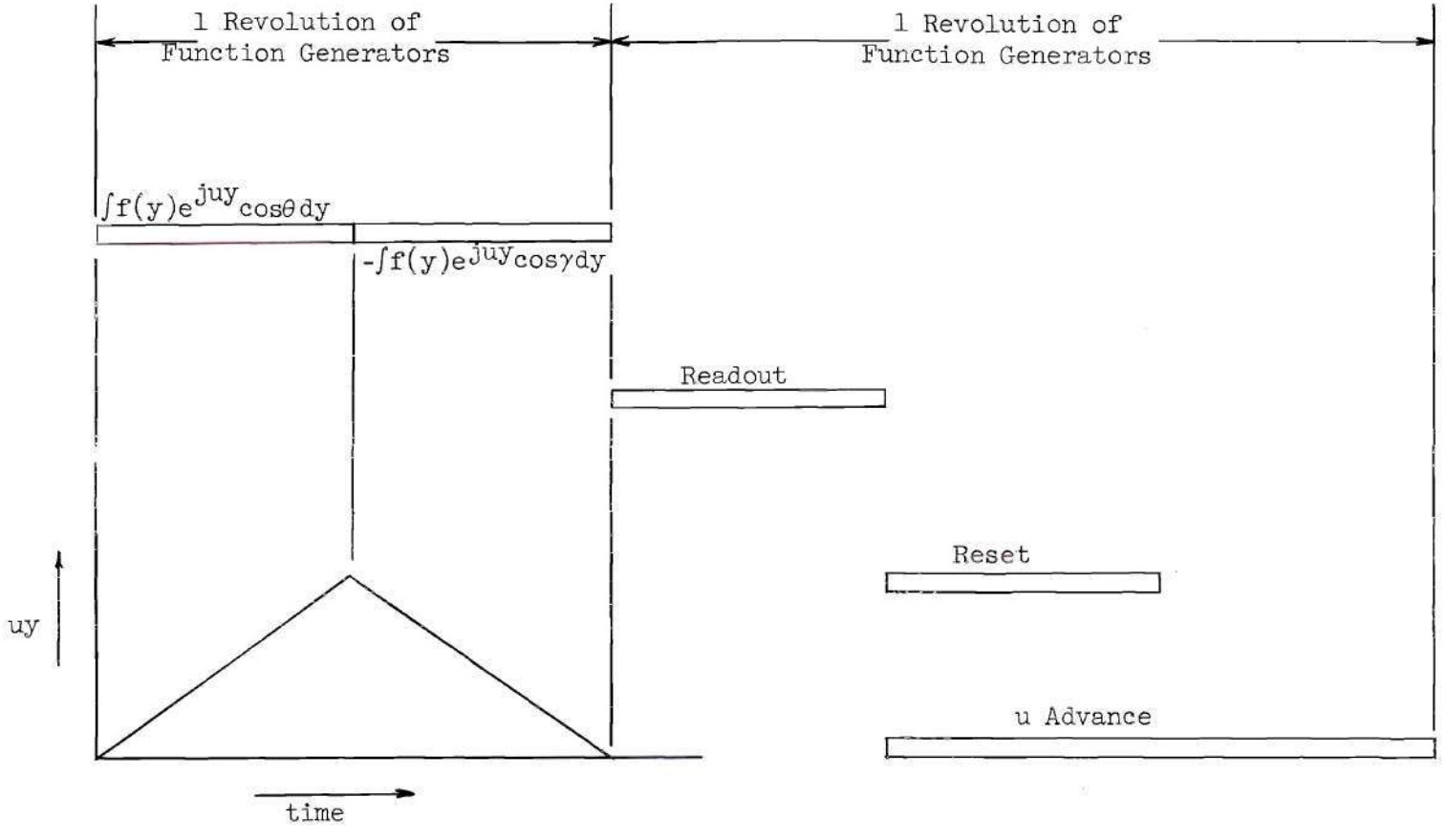

Figure 4. Timing Diagram and Plot of uy During Integration Period

of A(u) for one angular far-field direction. The first integral is computed during the first half of the integration period and stored; then the second integral is computed, added to the first, and read-out to the recorder. The integrators are then reset, the parameter u is changed to a value u + Δu and the next value of A(u) is computed. It is seen in Figure 3 that the slope of the uy function is reversed for the evaluation of the second integral; this allows the first integral to be integrated from the lower to the upper aperture extremity, and the second integral to be integrated from the upper to the lower extremity of the aperture. The function uy is simulated in the computer by an integrator with a constant voltage input which is proportional to u; the above procedure eliminates the necessity for resetting the uy integrator after the evaluation of the first integral.

Integration in the manner outlined above allows Equation 11 to be rewritten as

$$\overline{A(u)} = \int_{-a}^{a} \overline{f(y)} e^{juy} \cos\theta \, dy - \int_{a}^{-a} \overline{f(y)} e^{juy} \cos\gamma \, dy, \qquad (12)$$

which can be written

$$\overline{A(u)} = \int_{-a}^{a} f(y) e^{j\phi(y)} \cos\theta \, dy - \int_{a}^{-a} f(y)^{j\phi(y)} \cos\gamma \, dy, \qquad (13)$$

where $\phi(y) = uy + \psi(y)$, and where $\overline{f(y)} = f(y)e^{j\psi(y)}$. In rectangular form this becomes

$$\overline{A(u)} = \int_{-a}^{a} f(y) \cos\theta \cos\phi(y)\, dy + j\int_{-a}^{a} f(y) \cos\theta \sin\phi(y)\, dy \quad (14)$$

$$-\int_{a}^{-a} f(y) \cos\gamma \cos\phi(y)\, dy - j\int_{a}^{-a} f(y) \cos\gamma \sin\phi(y)\, dy.$$

The angle γ between a normal to the aperture and the direction of the Poynting vector at any point of the aperture must be calculated prior to any computation from

$$\gamma = \tan^{-1}\left(\frac{d\psi}{dy}\right). \quad (15)$$

The amplitude and phase function generators consist of split rotating wooden cylinders on which the required functions are placed with wire. The functions $f(y)$ and $\psi(y)$ are placed on corresponding halves of the amplitude and phase cylinders. The functions $f(y) \cos\gamma$ and $\psi(y)$ are placed on the remaining halves of the two drums.

Referring to Equation 14 and to Figure 4, a step-by-step account of the sequence of events which transpires during the computation of $A(u)$ for one particular far-field direction is given below.

During the first half of the integration period the circuits indicated by solid lines (Figure 3) are active, during the second half of the integration period the alternate circuits indicated by dashed lines are activated.

I. The First Half of the Integration Period

(a) Voltages proportional to the functions $f(y)$ and $\psi(y)$ are read into the computer.

(b) The voltage proportional to $f(y)$ is fed into a sine-cosine potentiometer and a voltage proportional to $f(y) \cos \theta$ is taken off.

(c) The voltage proportional to $\psi(y)$ and a voltage proportional to uy are fed into a summation circuit and a voltage proportional to $\phi(y)$ is taken off.

(d) The voltages proportional to $f(y) \cos \theta$ and $\phi(y)$ are fed to a resolver and voltages proportional to $f(y) \cos \theta \cos \phi(y)$ and $f(y) \cos \theta \sin \phi(y)$ are obtained.

(e) These voltages are fed to separate integrators and voltages proportional to the integrals $\int f(y) \cos \theta \cos \phi(y)\, dy$ and $\int f(y) \cos \theta \sin \phi(y)\, dy$ are stored in the integrators.

II. The Second Half of the Integration Period.

(a) Voltages proportional to $f(y) \cos \gamma$ and $\psi(y)$ are read into the computer.

(b) The voltages proportional to $f(y) \cos \gamma$ is fed into an inverter and a voltage proportional to $-f(y) \cos \gamma$ is obtained.

(c) Again the voltage proportional to $\psi(y)$ and a voltage proportional to uy are fed to a summation circuit and a voltage proportional to $\phi(y)$ taken off.

(d) Voltages proportional to $-f(y) \cos \gamma$ and $\phi(y)$ are fed to a resolver and voltages proportional to $-f(y) \cos \gamma \cos \phi(y)$ and $-f(y) \cos \gamma \sin \phi(y)$ are obtained.

(e) These voltages are fed into separate integrators and integrated.

(f) At the end of the second half of the integration period voltages proportional to $\left[\int f(y) \cos \theta \cos \phi(y)\, dy - \int f(y) \cos \gamma \cos \phi(y)\, dy\right]$

and $\left[\int f(y) \cos\theta \sin \phi(y) - \int f(y) \cos\gamma \sin \phi(y)\right]$ are stored in the integrators. These voltages are fed to the quadrature summation circuit where they are displaced in phase 90°and summed.

(g) This voltage which is proportional to A(u) is then plotted on an antenna pattern recorder in decibels.

The outputs of the real and imaginary integrators of this computer are connected to the x and y axes respectively of an oscilloscope as shown in Figure 3. When an oscilloscope of fairly long persistence is used this arrangement yields an instantaneous visual picture of the Fraunhofer spiral* for each far-field angular direction θ.

In addition a marker generator is provided as an aid for determining the portion of the aperture phase function, $\psi(y)$, which is mainly responsible for the energy contributions in each far-field direction. This marker generator provides a voltage pulse which can be made coincident with any desired point on the phase function generating drum. The voltage pulse is utilized to modulate the z-axis of the oscilloscope and thus provides a bright spot which can be positioned to any desired portion of the oscilloscope presentation. When the marker is positioned to the relatively straight portion of the Fraunhofer spiral (which corresponds to that portion of the aperture from which energy arrives at the field point under consideration with small phase differences) it will indicate the portion of the aperture which is mainly responsible

---

*The phasor summation of energy contributions from all elements of an aperture to a particular far-field point. These curves, which are known as vibration curves in optics, have been termed "Fraunhofer spirals" by personnel of the Georgia Institute of Technology because they describe the radiation characteristics of an antenna in the Fraunhofer (far-field) region.

for the magnitude of the far-field radiation pattern at that particular field point. This allows one to calibrate the computer solution in terms of the phase function which produced it.

The Existing Computer.--This computer determines the absolute value A(u) of the integral

$$\overline{A(u)} = \int_{-a}^{a} \overline{f(y)} e^{juy} dy, \tag{17}$$

which can be written

$$\overline{A(u)} = \int_{-a}^{a} f(y) e^{j\phi(y)} dy, \tag{18}$$

where $\phi(y) = uy + \psi(y)$, and $\overline{f(y)} = f(y)e^{j\psi(y)}$. In rectangular form, the integral becomes

$$A(u) = \int_{-a}^{a} f(y) \cos \phi(y)\, dy + j \int_{-a}^{a} f(y) \sin \phi(y)\, dy. \tag{19}$$

A block diagram of this computer is shown in Figure 5; circuit operations are indicated on the diagram. The function generating cylinders are not split and only one function is placed on each drum.

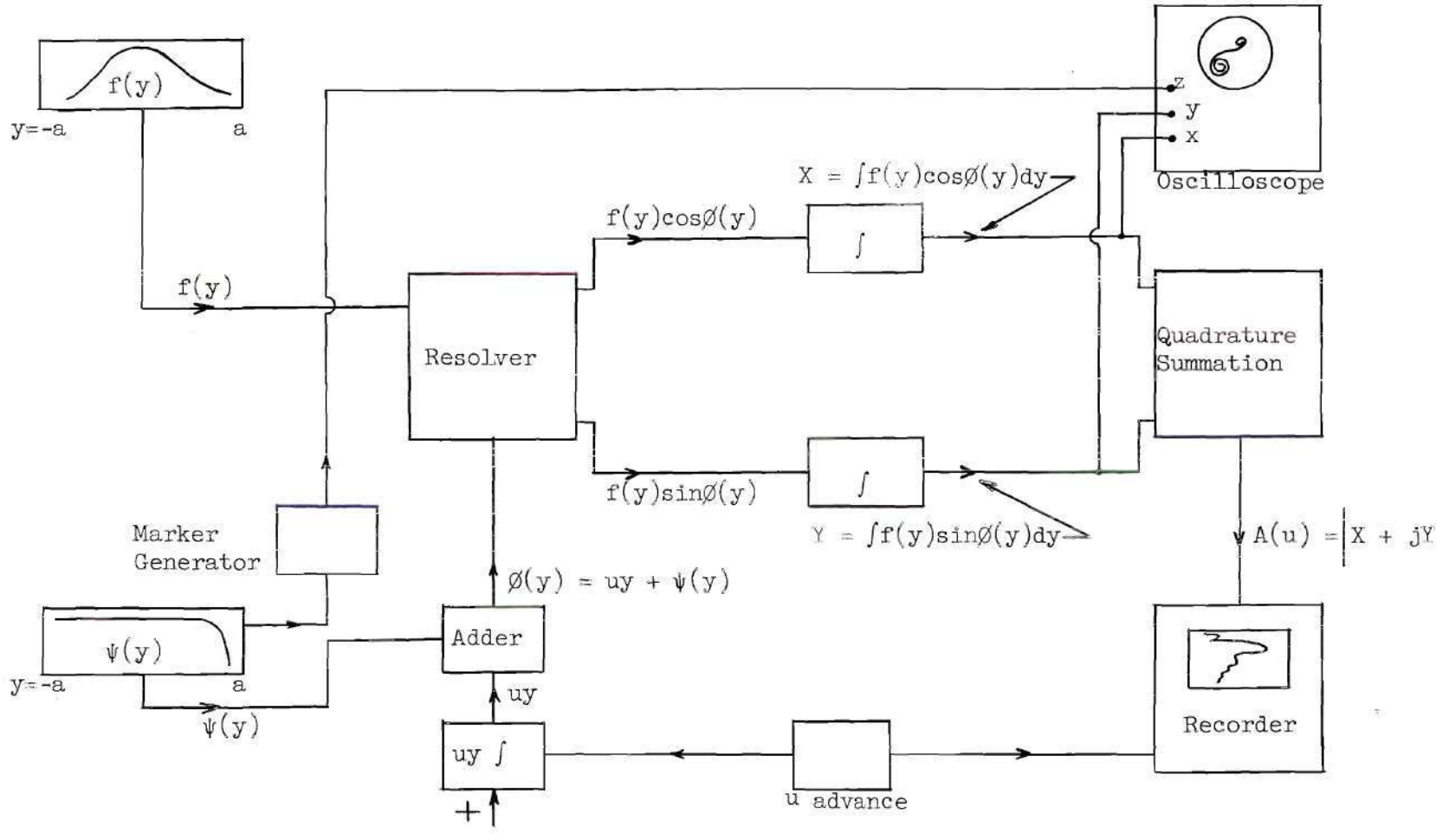

Figure 5. Existing Computer

CHAPTER IV

METHOD OF SOLUTION

Assuming that the necessary analog computer equipment is available, this method of finding a microwave reflecting surface for beam-shaping is equally applicable to the general relation between the aperture-field and far-field (Equation 8) and to the narrow beam approximation (Equation 10). The experimental evidence offered in Chapter V is a problem solution in which the narrow beam approximation was applicable; for this reason the discussion of the method of solution in this chapter is in terms of the narrow beam approximation. It should be remembered, however, that this implies no limitation of the method.

The narrow beam approximation is given by

$$\overline{A(u)} = \overline{K} \int_{-a}^{a} f(y)\, e^{j\left[uy+\psi(y)\right]} dy, \qquad (20)$$

where $uy + \psi(y) = \phi(y)$. The phase function uy is the ordinary phase function which results in the diffraction phenomenon. $\psi(y)$ is the aperture phase function which can be controlled by the shape of the reflector surface.

It can be shown from Equation 20 that, if it is desired to prevent a pattern from "lobing out" in a particular region, it is necessary to produce an aperture phase function $\psi(y)$ which decreases the rate of

change of $\phi(y)$ in that region. In this chapter a method for finding a microwave reflecting surface which will cause $\phi(y)$ to vary in a desired and a predictable fashion is described.

The Far-Field Pattern.--Usually the given specification of a beam-shaping problem is the required shape of the far-field pattern. Given this shape, the problem is to find a microwave reflecting surface which will physically produce this distribution of energy in the far-field.

An ideal shaped-beam pattern would conform smoothly to the desired pattern inside the region of interest and decrease discontinuously to zero outside the region of interest. This pattern cannot be obtained practically because diffraction causes fluctuations of the pattern shape in the shaped-beam region and because an aperture of infinite dimensions would be required to cause a pattern to decrease to zero discontinuously. As an engineering compromise the beam-shaping surface is normally attached to either the upper or lower extremity of a pencil-beam-forming parabolic surface. This parabolic section causes the energy level to decrease more rapidly outside the region of interest than would the beam-shaping section alone. The amplitude of the aperture illumination function at the edge of the aperture opposite to the beam-shaping section control the magnitude of the fluctuations in the shaped-beam region of the pattern (see Appendix I). A small amplitude at this edge causes a small fluctuation and a larger amplitude causes larger fluctuations in the pattern.

In Figure 6 the superposition of patterns from a beam-shaping surface and from a pencil-beam forming surface is shown for a typical microwave antenna.

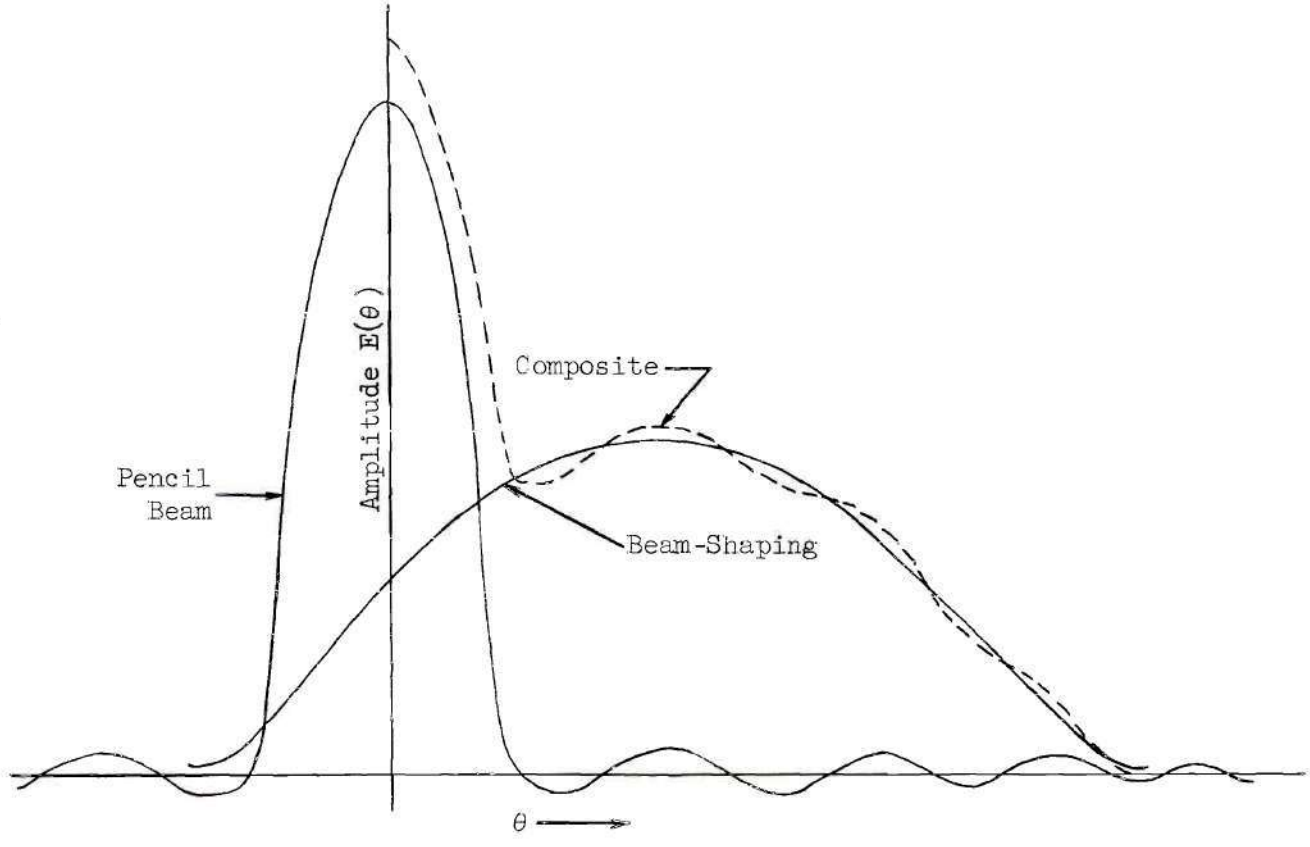

Figure 6. The Structure of a Shaped-Beam Pattern

The Amplitude Illumination Function

The aperture illumination function, $\overline{f(y)} = f(y)e^{j\psi(y)}$, describes the distribution of energy in the aperture with regard to amplitude and phase. When given this function as data, the analog computing equipment described in Chapter III calculates the resulting far-field pattern. This section describes the techniques employed in obtaining the amplitude and phase of the aperture illumination function.

The Amplitude Function.--The amplitude of the illumination function is obtained by modifying the amplitude of the primary-feed radiation pattern by a factor of $1/\sqrt{\rho}$ (11), where ρ is the distance from the center of phase of the primary feed to the reflector surface. The square-root of ρ is used because all problems are two dimensional when using this method.

At the beginning of a problem, the exact position of the beam-shaping surface is not known and therefore the exact amplitude of the illumination function cannot be found. It has been shown (12), by employing near-zone analog computing equipment, that the method outlined below for finding the amplitude function is sufficiently accurate for most purposes.

To illustrate this method, consider Figure 7 which depicts a beam-shaping surface AB attached to the lower extremity of a pencil-beam-forming parabolic section at point A. The amplitude function is first calculated by assuming that the entire surface is parabolic, as indicated by the dashed curve, with aperture limits of y_o and y_n. The aperture is then elongated until it contains the extreme ray of interest, R_n. Finally, the amplitude function is lengthened to encompass the new

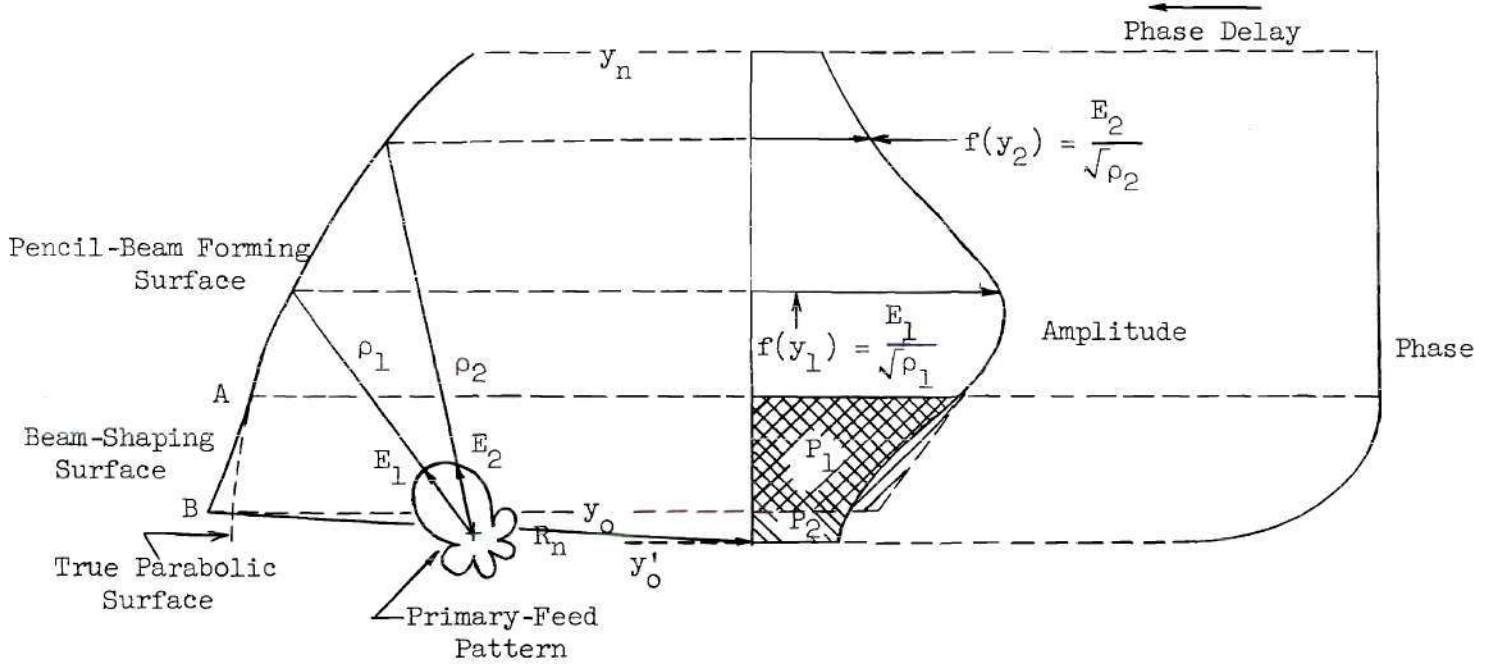

Figure 7. On the Method of Obtaining the Amplitude and Phase of an Illumination Function

aperture described by the aperture limits y'_o and y_n; but the power level contributed by the beam-shaping surface is lowered so that $P_1 = P_2$ in Figure 7.

The Phase Function.--Since microwave antennas lend themselves, to a first order of approximation, to analysis by geometrical optics, the general shape of the phase of the illumination function is known. For the case of Figure 7 the energy from the beam-shaping surface is directed downward below the peak of the beam. To accomplish this the energy from the beam-shaping surface must lag, in phase, the energy from the pencil-beam-forming surface. A typical phase function for this situation is shown in Figure 7. Conversely, if energy from the beam-shaping surface is to be directed upward above the beam peak it must lead, in phase, the energy from the pencil-beam-forming surface.

It is also known that relatively small phase changes are required over the beam-shaping aperture in order to shape the far-field pattern over narrow angular regions and that larger phase changes are required for shaping over wider angular regions.

Thus, the required phase function is obtained in the following manner:

(a) With proper regard to the properties outlined in the preceding paragraphs, a phase function is assumed.

(b) This phase function and the amplitude function, which is found by the process described in the preceding section, are fed into the analog computer as data.

(c) The computer then plots the far-field radiation pattern which results from this aperture energy distribution.

(d) At the same time that the resulting radiation pattern is being plotted, the marker generator in the computer is utilized to calibrate the pattern's angular scale (as described in Chapter III) so that the portion of the aperture which contributes energy into each far-field direction is known.

(e) The resulting pattern will deviate from the desired beam-shape; in some regions the energy level will be too high and in others it will be too low. To alter the energy level in a particular far-field direction, it is merely necessary to observe (from the calibration of part d above) which portion of the phase function is causing energy to be propagated in the direction under consideration. Then to raise the energy level, the slope of the phase function in the region of the aperture which is contributing energy in this direction is maintained over a larger portion of the aperture. To lower the energy level in this direction, the slope of the phase function in this region is maintained over a smaller portion of the aperture.

(f) Using the criteria of part (e), the initial phase function is modified as necessary in all regions; thus, a new phase function is obtained. Then the entire process, beginning with part (b) is repeated.

Experience has shown that a required phase function can be found in approximately three to four trials by a skilled operator.

The Elliptic Intersection Method of Obtaining a Beam-Shaping Surface.-- After the required phase function has been found, the surface required to obtain this phase is then found by employing the Elliptic Intersection Method. The Elliptic Intersection Method is a geometrical optics approximation. Geometrical optics assumes that the amplitude and phase of the energy at a particular aperture point is derived from a single point on the surface of the reflector. This is not completely true since the amplitude and phase at any given aperture point is due to the integrated effect, with proper regard to amplitude and phase, of contributions from all portions of the reflector surface. This situation is illustrated in Figure 8 with a Cornu spiral. It can be shown that the angle δ between the actual phase and the phase given by geometrical optics is negligible for the purposes here.

The Elliptic Intersection Method is discussed in terms of a problem such as the one illustrated in Figure 7; the lower portion of this sketch is expanded and redrawn in Figure 9. The center of phase of the primary feed is located at point O, the focus of the parabolic section. The phase at any point along the aperture is a function of the distance $OP_n y_n$; the phase along the aperture described by the parabolic section is a constant and a function of the distance OAA'. Let the phase shift equivalent of OAA' be called $\zeta(A)$; then the required phase at any aperture point, such as y_1, can be expressed as $\psi(y_1) = \zeta(A) + \beta(y_1)$ where $\psi(y_1)$ is the value of the aperture phase function at y_1. Many elemental surfaces which will physically realize the required phase at each aperture point can be specified mathematically.

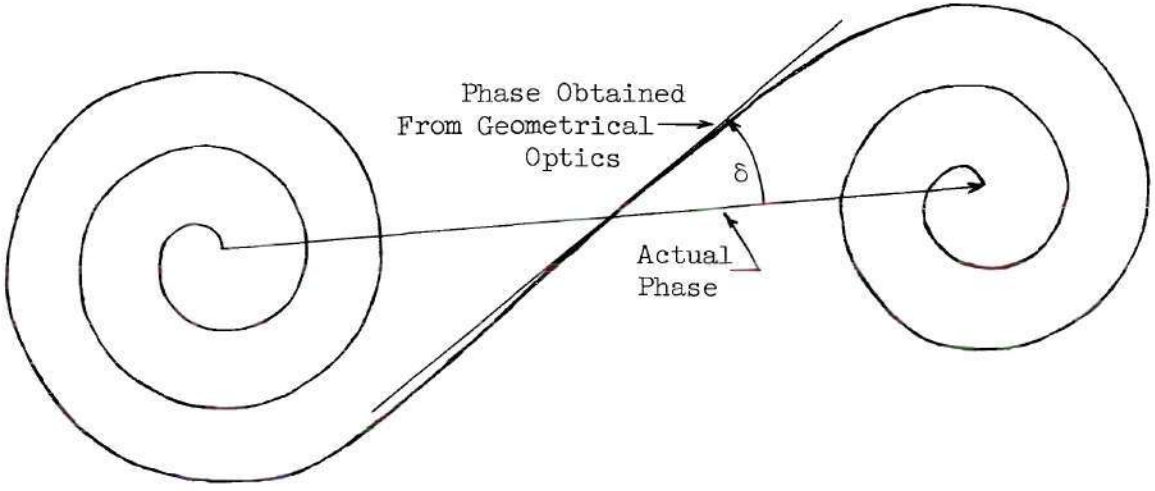

Figure 8. Illustration of Phase Approximation

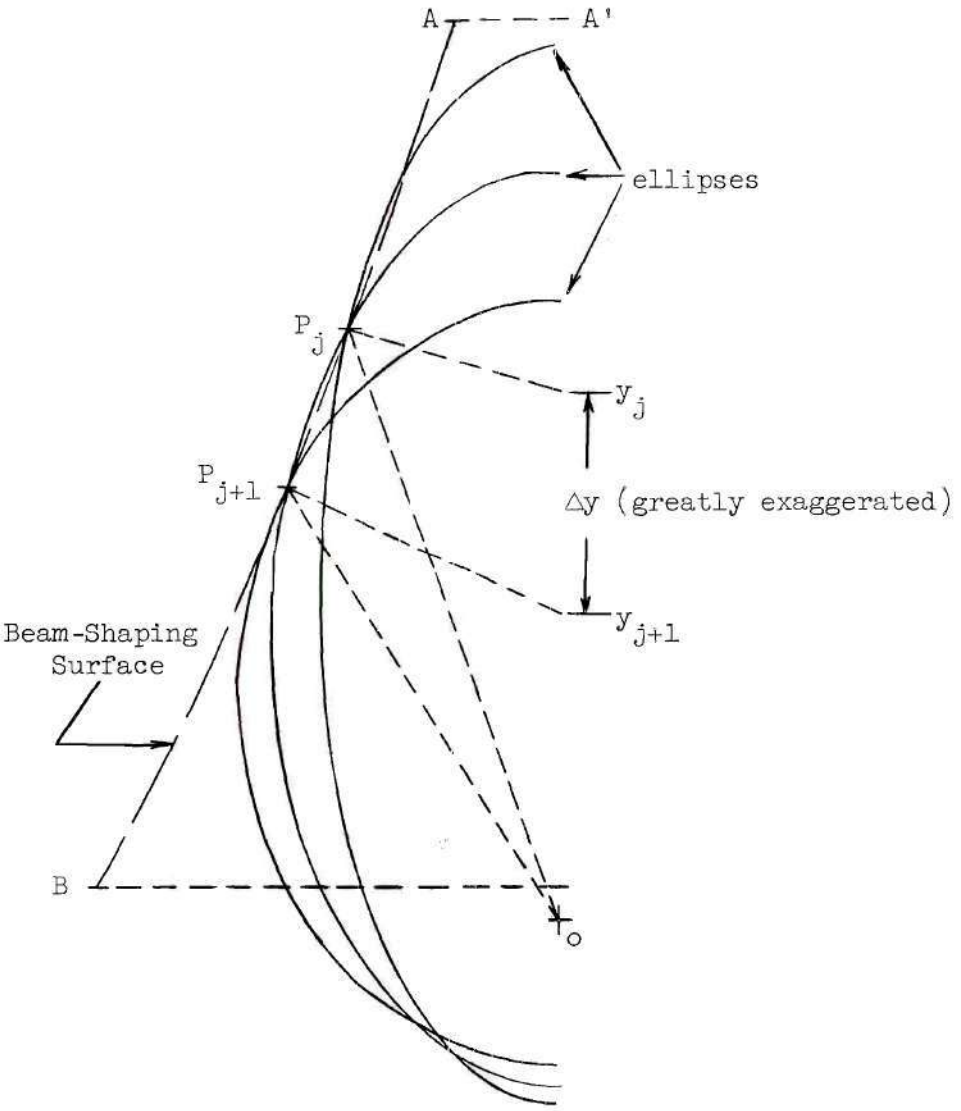

Figure 9. On the Elliptic Intersection Method

An ellipse with foci at point 0 and the aperture point in question is particularly applicable for this purpose because the polar generator of an ellipse is constant in length. Therefore, if the polar generator has the proper phase shift equivalent, $\psi(y)$, for a particular aperture point, y, then every point on the elliptic surface described by this polar generator also has the proper phase at this aperture point. Consider an ellipse with foci at 0 and y_1 and a polar generator with a phase shift equivalent (distance in wavelengths) of $\psi(y_1) = \zeta(A) + \beta(y_1)$. For $y = y_1 + \Delta y = y_2$, there exists an ellipse with foci 0 and y_2 having a polar generator with a phase shift equivalent of $\psi(y_2) = \zeta(A) + \beta(y_2)$. At aperture point $y_3 = y_2 + \Delta y$ there exist still another ellipse having a polar generator with a phase shift equivalent of $\psi(y_3) = \zeta(A) + \beta(y_3)$ etc.

In this method the required microwave reflecting surface is taken as the locus of the intersection points of a number of ellipses such as those described in the preceding paragraph. The locus of these intersection points can be made sufficiently close to the required surface by choosing Δy sufficiently small.

The phase shift $\zeta(A) + \beta(y_n)$ determines the size of the ellipse; the size of the ellipse and the distance between foci determines the eccentricity with which the equation of the ellipse can be determined. (See Appendix II).

Calculation of the intersection points is greatly facilitated by using digital computing equipment.

CHAPTER V

SAMPLE PROBLEM

The Problem.--The problem which is employed to verify this method of beam-shaping is the design and construction of an antenna consisting of a section of a parabolic cylinder with a beam-shaping surface attached at its lower extremity (such as the one shown in Figure 7). The beam-shaping surface is to encompass approximately one-fourth of the total vertical dimension of the reflector. The radiation pattern of the antenna, in the plane of shaping, is to have a modified $\csc^2\theta$ shape (as shown by the short dashed lines in Figure 15) out to an angle of fifteen times its half-power beamwidth. The side lobe suppression (on the side of the radiation pattern opposite to the shaped beam portion) is to be greater than 18 db below the peak intensity of the beam.

The Solution of the Problem.--The primary feed horn was designed* and its radiation pattern was measured. The dimensions of the horn, in wavelengths are shown in Figure 10(a). The radiation pattern measured for this horn as constructed is shown in Figure 10(b).

---

*Normally the primary feed horn is designed prior to the beginning of any beam-shaping calculations; it is possible, with sufficient experience, to assume a primary feed pattern and then to design a horn with these characteristics later on.

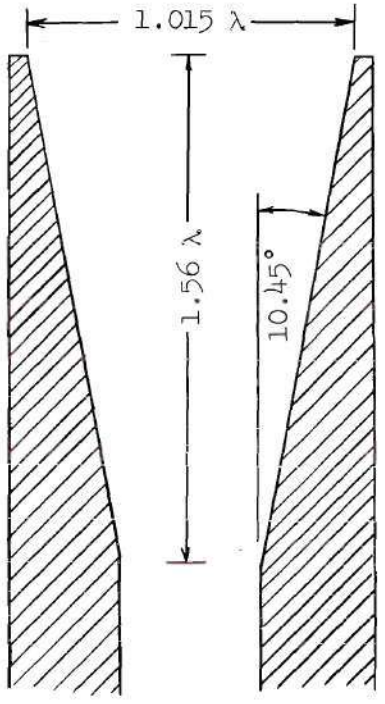

(a)

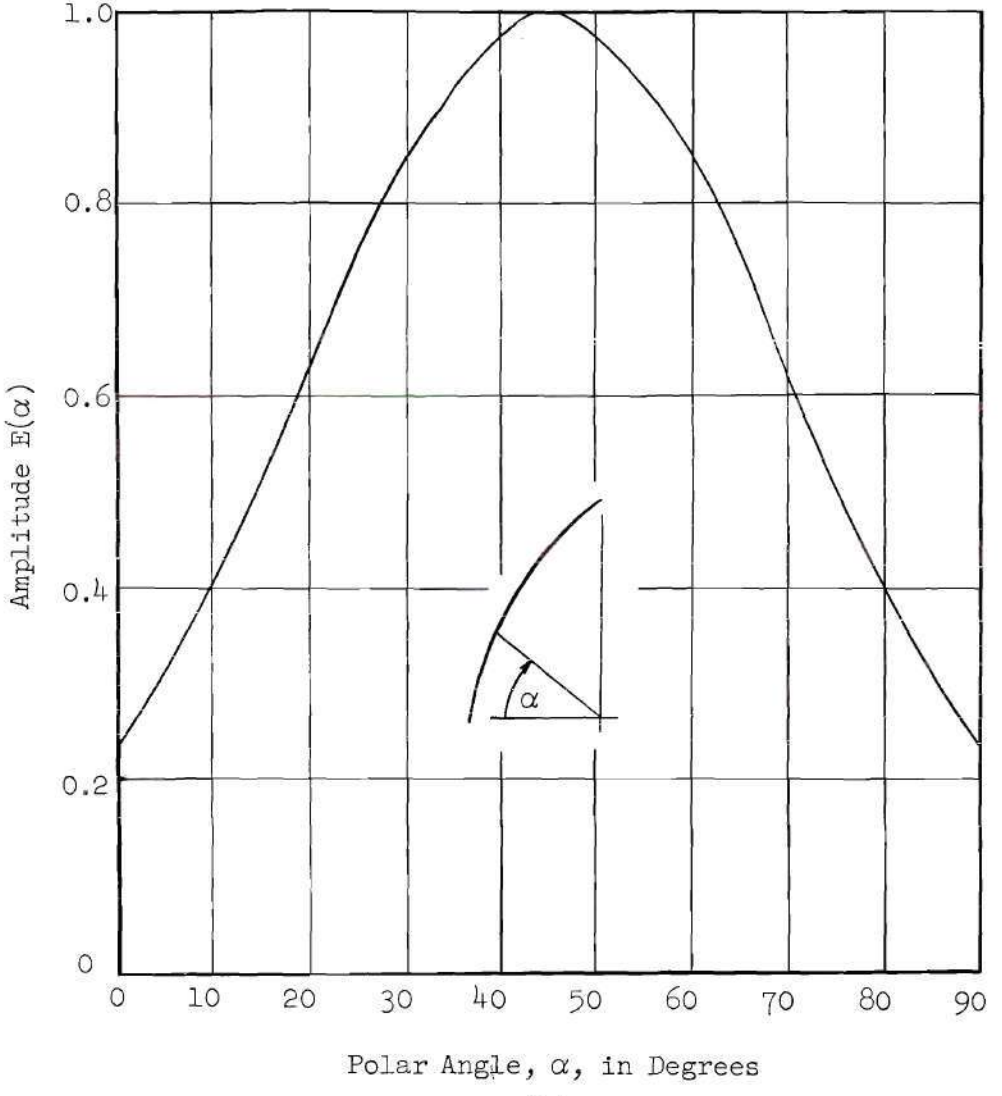

(b)

Figure 10. The Dimensions and the Radiation Pattern of the Primary Feed

From the measured primary feed pattern the amplitude of the aperture illumination function was derived using the technique outlined in Chapter IV. The amplitude function which was found is shown in Figure 11; the dashed curve is the amplitude function which would result if the entire reflecting surface was parabolic. The solid curve shows the amplitude function which was used; it has been lengthened and lowered in the beam-shaping region to account for the apparent stretching of the aperture due to beam-shaping.

In Figure 12 the phase of the aperture illumination function which was found by the technique described in Chapter IV is shown. The amplitude of the aperture illumination function and the desired far-field radiation pattern of the antenna under consideration are known. The known amplitude function and a series of trial phase functions were fed into the existing analog computer (described in Chapter III) as data. The required phase function was then taken as the trial phase function which yielded the desired far-field pattern from the computer.

The computer solution for this problem is shown in Figure 13. The antenna pattern recorder, on which this data was plotted, is designed to operate from a square-law detector. The output of the computer to the recorder is a voltage such that the ordinates of this curve must be doubled (on a graph linear in decibels) for comparison with experimental patterns.

The dimensions, in wavelengths, of the resulting experimental reflector are shown in Figure 14. The coordinates of the beam-shaping

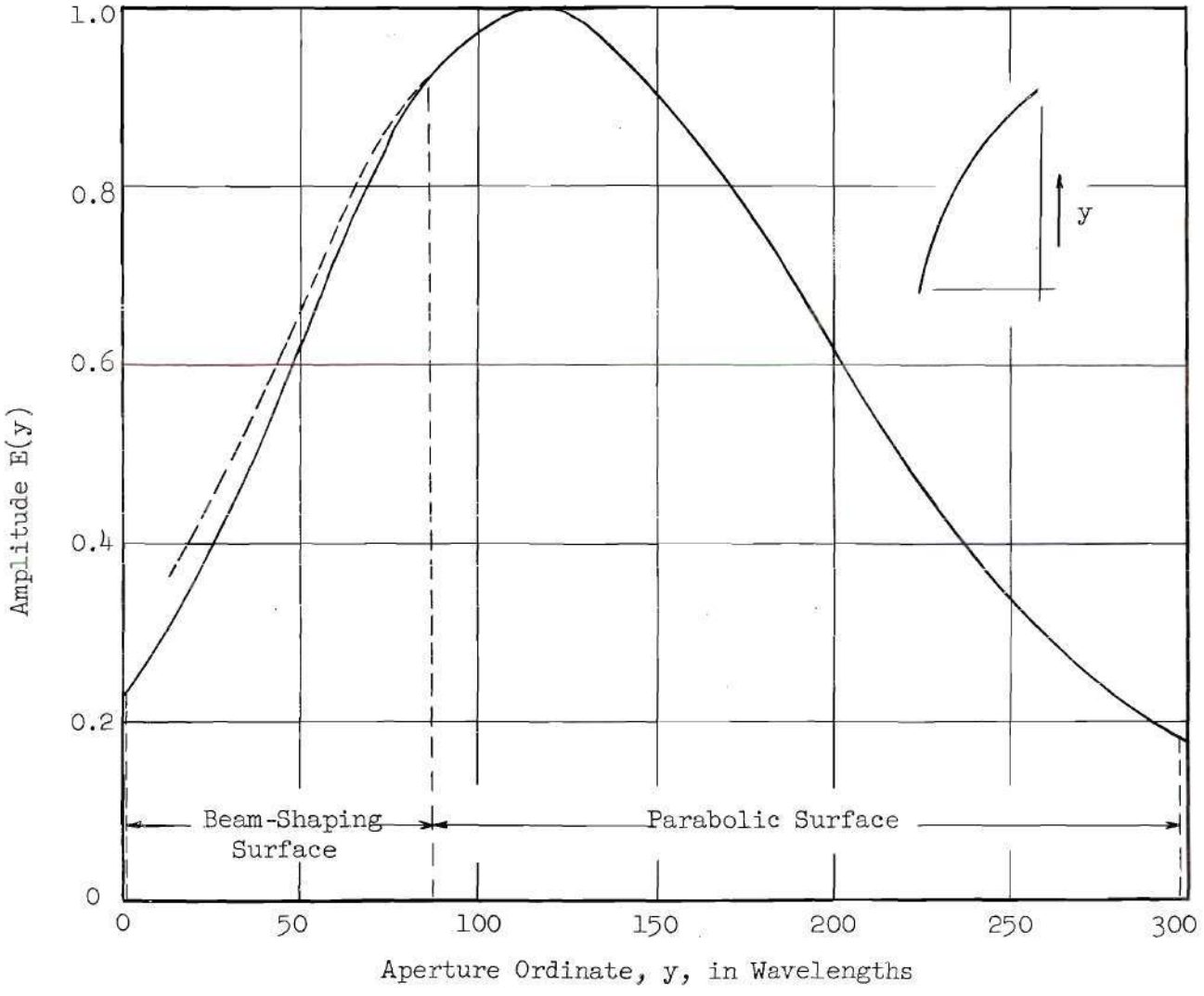

Figure 11. The Amplitude of Aperture Illumination Function

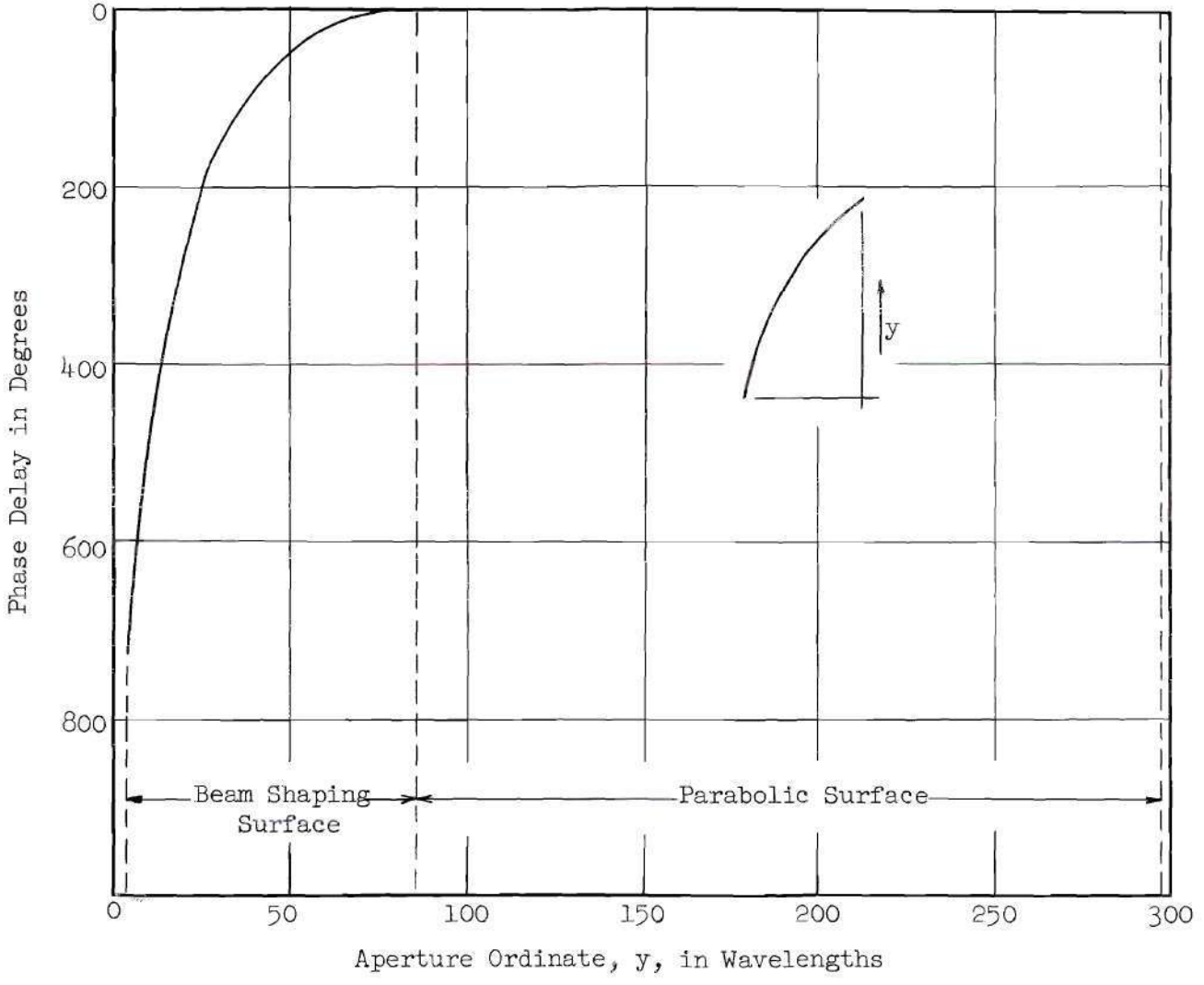

Figure 12. The Phase of the Aperture Illumination Function

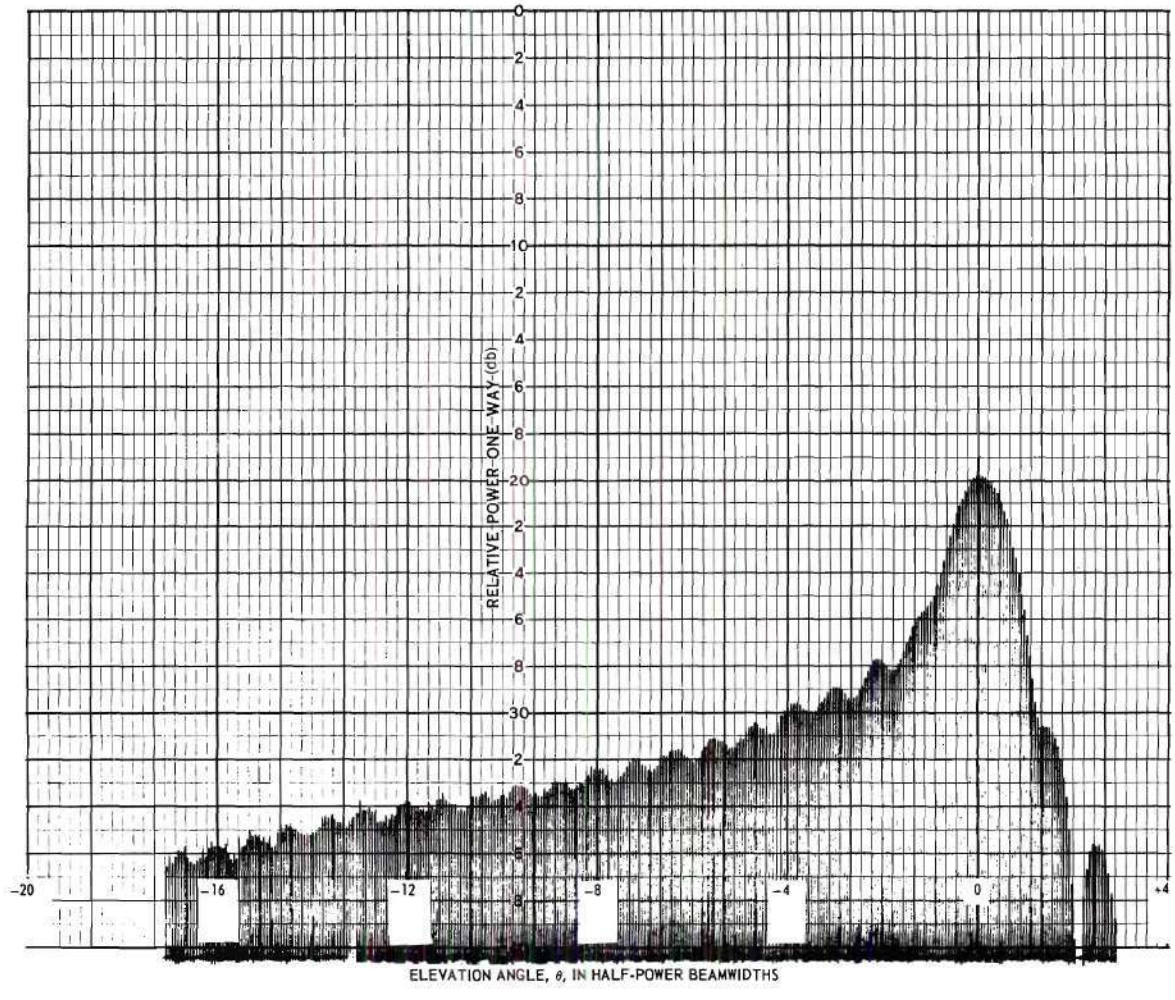

Figure 13. The Analog Computer Solution.

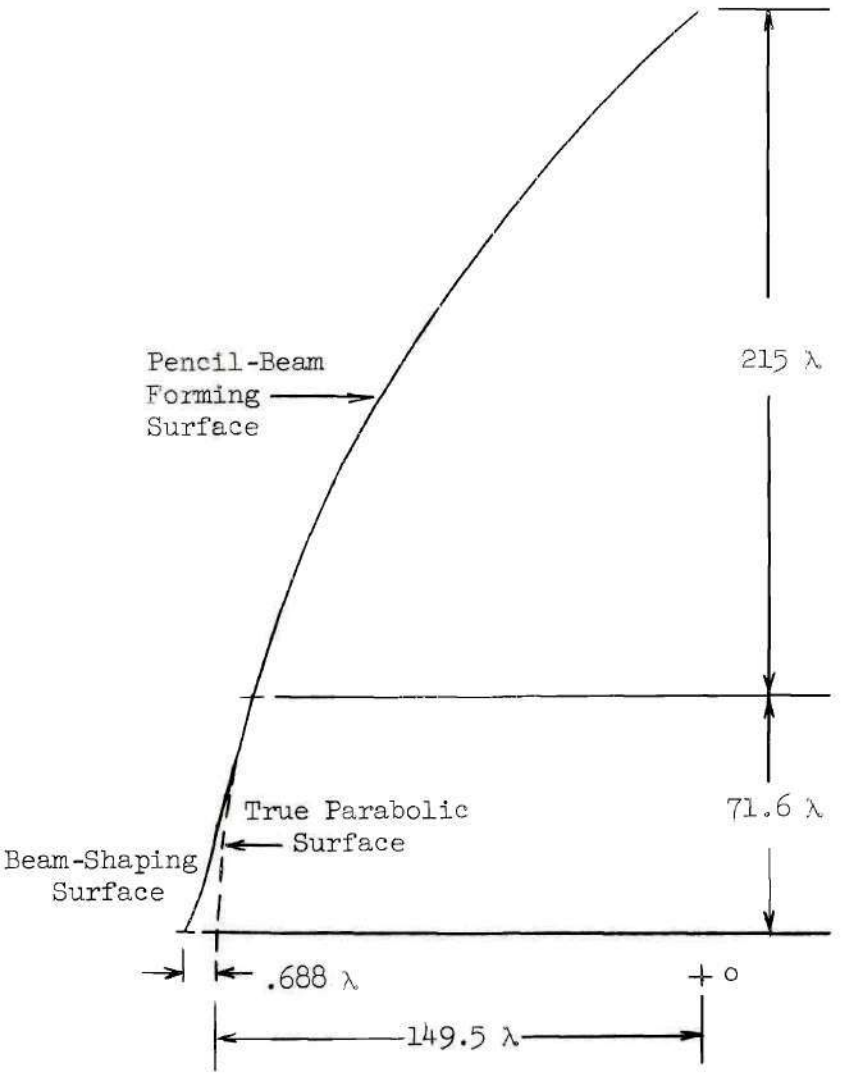

Figure 14. The Experimental Reflector

surface were found using the "Elliptic Intersection Method" which is described in Chapter IV. An I.B.M. 650 digital computer was programmed and utilized to facilitate these calculations.

In Figure 15 a comparison between the ideal, calculated, and experimental radiation patterns for this antenna are given.

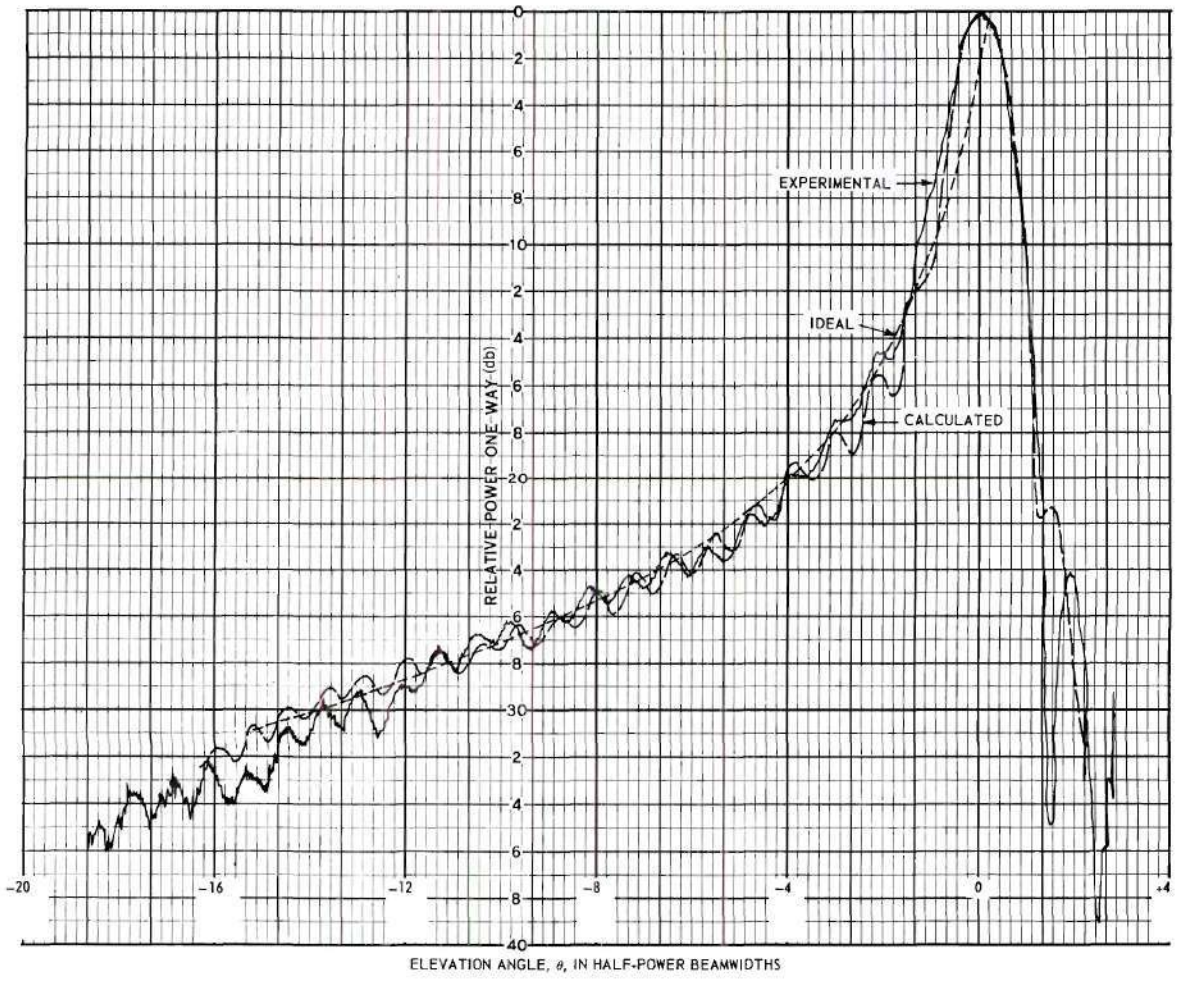

Figure 15. Comparison of Ideal, Calculated and Experimental Radiation Patterns.

CHAPTER VI

CONCLUSIONS AND DISCUSSION OF RESULTS

The work described in this thesis demonstrates the practicability of analog computer techniques in the solution of microwave antenna beam-shaping problems. Computers such as the ones described in Chapter III are relatively inexpensive to construct and they are very simple to program. Much costly machine shop work and experimental pattern range work is eliminated through their use in the determination of a surface to produce a desired shaped-beam pattern.

A study of Figure 14 reveals a variance, between the calculated and the experimental patterns, of no more than 2 db over the shaped beam region. This maximum variation occurs at a level which is greater than 30 db below the peak intensity of the beam. At this level, a 2-db variation represents an error of less than 0.04 per cent compared to the peak intensity. Accuracy of this kind is more than sufficient for most problems.

Most of the errors which are inherent in this method stem from the geometrical optics approximations which are made. The amplitude of the aperture illumination function is calculated as if the amplitude at a particular aperture point is due to energy contributions from a single point on the reflector. The reflector surface is obtained, from the phase of the aperture illumination function, by employing the "Elliptic Intersection Method" which assumes that the phase at each aperture

point is due to a single point on the reflector. As previously pointed out, this is not rigorously true because the amplitude and phase of the energy at any aperture point is due to the summation of contributions from all portions of the reflector. It has been shown during the course of this work, as indicated by the experimental results, that these errors are not appreciable in the microwave region.

A P P E N D I C E S

APPENDIX I

FLUCTUATIONS IN THE SHAPED REGION OF A PATTERN

Figure 16(a) depicts a microwave aperture with the amplitude and phase of its illumination function shown as a function of aperture position. It is evident, from the phase plot, that the lower portion of this aperture is utilized for beam-shaping. In the following paragraphs it is shown that the magnitude of the fluctuations in the shaped region of the far-field radiation pattern from such an aperture is controlled by the amplitude of the illumination function near the upper extremity of the aperture.

A typical Fraunhofer spiral for the energy at a far-field point P_1 in a direction θ_1 is shown in Figure 16(b). The spiral is composed of three general regions: the relatively straight central region, the tightly spiraled end on the right, and the more loosely spiraled end on the left. The relatively straight central section of the spiral is due to that portion of the aperture from which energy arrives at the field point P_1 with small differences in phase. It is obvious that this portion of the aperture is responsible for the major part of the resultant field magnitude at P_1. The tightly spiraled end on the right is the result of contributions from the remainder of the beam-shaping aperture. This portion of the curve is tightly wound because the relative phase of contributions from this area is changing rapidly as a result of the intentional phase variation which is inserted to

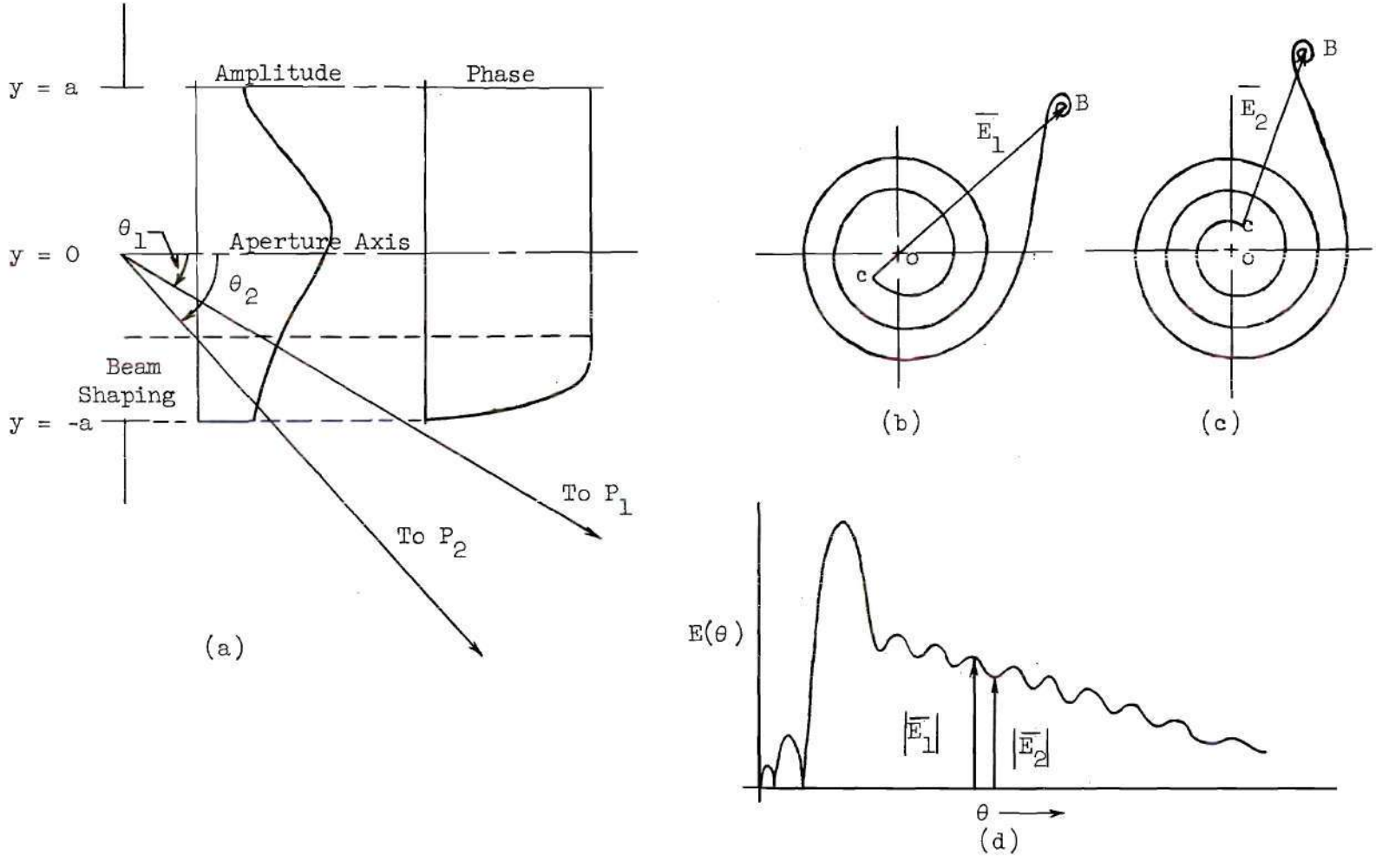

Figure 16. Amplitude Fluctuations in the Shaped Region of a Pattern

accomplish beam-shaping. The more loosely spiraled end of the curve on the left is produced primarily by the constant phase portion of the aperture. The relative phase between contributions from this area is a result of the fact that field point P_1 is not located on the aperture axis. The initial offset OC to the starting point of the spiral is due to the amplitude of the illumination function at the upper edge of the aperture; if this amplitude were zero, the curve should spiral in to the point O. The resultant far-field amplitude, in the θ direction, is given by the phasor $\overline{E}_1$ connecting the points C and B. If the field is investigated for various values of the angle θ, it will be seen that the point C will describe a circular path about the point O as θ varies. For the case shown, the points C and B are on opposite sides of the point O; this orientation produces a maximum in the fluctuations in the shaped-pattern region. In some other far-field direction, such as θ_2, the Fraunhofer spiral will appear as shown in Figure 16(c). It is seen that the relative phase of the contributions has changed such that the points C and B are now on the same side of the point O; this orientation produces a minimum in the shaped pattern. A typical relationship between these two spirals and a far-field pattern is shown in Figure 16(d).

The end point B of the tightly spiraled portion of the curve describes a circular path about its origin in the same manner as does the point C. However, this region of the curve is spiraled so tightly that the small change in relative location experienced by B has negligible effect on the pattern. Therefore it is seen that the amplitude OC of the illumination function at the upper aperture extremity controls the magnitude of the fluctuations in the shaped region of the pattern.

APPENDIX II

THE ELLIPTIC INTERSECTION GEOMETRY

The Ellipse.--The polar equation of an ellipse is (13)

$$r(\theta) = \frac{ep}{1-e\cos\theta}, \text{ for } o<e<1, \tag{21}$$

where e is the eccentricity of the ellipse which is given by

$$e = \frac{y}{2a}. \tag{22}$$

The parameters contained in these equations are illustrated in Figure 17. The distance $r(\theta)+r'$ is a constant (invariant with θ) and is the phase shift experienced by energy which is emitted at point O and arrives at point O' after being reflected at the elliptical surface. This distance is always equal to 2a; thus, an ellipse, whose polar generator [the distance $r(\theta)+r'$] has any desired phase, is obtained when

$$2a = 2f \pm \Delta\psi \frac{\lambda}{360} \tag{23}$$

where

f is the focal length of the parabolic surface to which the beam-shaping surface is attached,

and $\Delta\psi$ is the phase variation in degrees required at the aperture point in question.

The Intersection of Two Ellipses.--Consider the two intersecting ellipses shown in Figure 18. Their focal points at the point O coincide

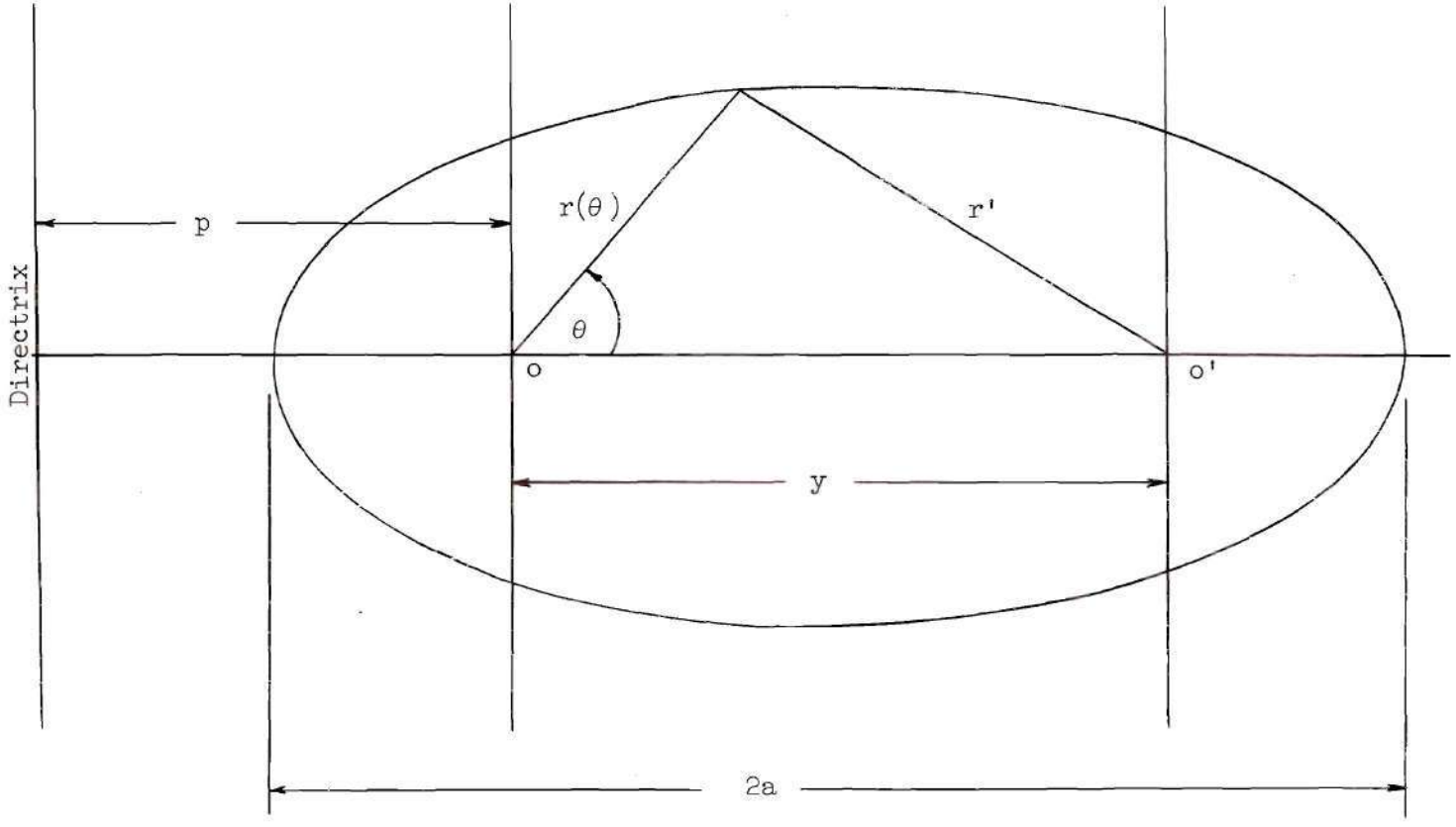

Figure 17. The Elliptic Geometry

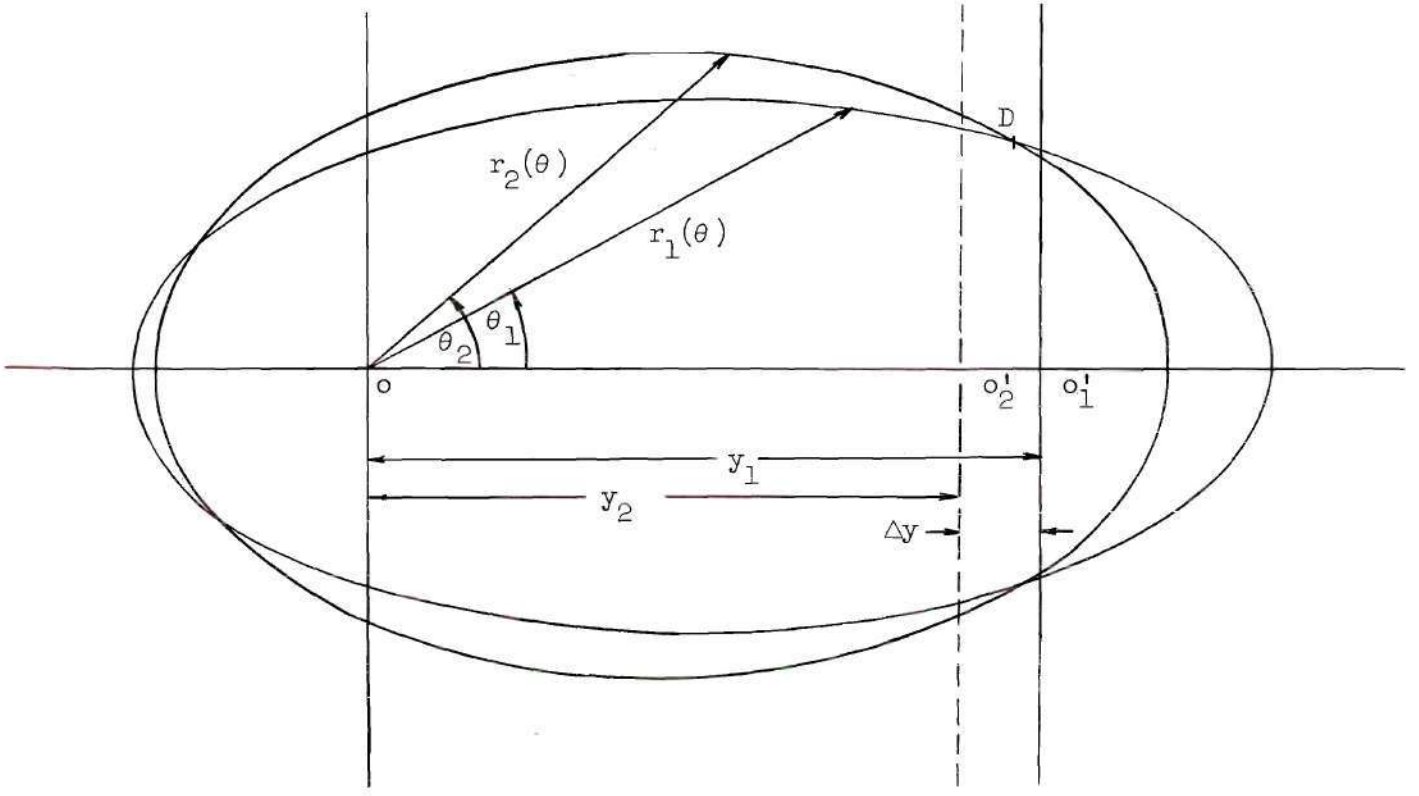

Figure 18. Two Intersecting Ellipses

whereas their remaining focal points are displaced from each other by an amount Δy. The equations of the two ellipses are

$$r_1(\theta) = \frac{e_1 p_1}{1-e_1 \cos \theta_1} \tag{24}$$

and

$$r_2(\theta) = \frac{e_2 p_2}{1-e_2 \cos \theta_2}. \tag{25}$$

The ellipses intersect at four points; the point described by the smallest positive value of the angle θ (point D) is utilized here in obtaining the required surface.

At the point where the two curves intersect

$$r_1(\theta) = r_2(\theta) = r(\theta), \tag{26}$$

and

$$\theta_1 = \theta_2 = \theta. \tag{27}$$

Therefore

$$\frac{e_1 p_1}{1-e_1 \cos \theta} = \frac{e_2 p_2}{1-e_2 \cos \theta}, \tag{28}$$

or
$$e_1 p_1 - e_2 e_1 p_1 \cos \theta = e_2 p_2 - e_1 e_2 p_2 \cos \theta \tag{29}$$

and
$$e_1 e_2 (p_2 - p_1) \cos \theta = e_2 p_2 - e_1 p_1, \tag{30}$$

which finally yields

$$\cos\theta = \frac{e_2p_2 - e_1p_1}{e_1e_2(p_2 - p_1)} . \tag{31}$$

The rectangular coordinates of the intersection point are

$$x = r \sin\theta \text{ and} \tag{32}$$

$$y = r \cos\theta \tag{33}$$

where

$$r = \frac{e_1p_1}{1 - e_1 \cos\theta} = \frac{e_2p_2}{1 - e_2 \cos\theta} , \tag{34}$$

and

$$\sin\theta = \sqrt{1 - \cos^2\theta} . \tag{35}$$

Calculation of the intersection points is facilitated by rewriting Equation 31 as

$$\cos\theta = \frac{e_2p_2 - e_1p_1}{e_1(e_2p_2) - e_2(e_1p_1)} , \tag{36}$$

and observing from Figure 16 that

$$r(0) + r(\pi) = 2a \tag{37}$$

or

$$\frac{ep}{1-e} + \frac{ep}{1+e} = 2a \tag{38}$$

and

$$\frac{2ep}{1-e^2} = 2a, \tag{39}$$

which yields

$$ep = a(1-e^2). \tag{40}$$

Equation 40 makes the ep quantities and consequently the cos θ term of Equation 36 relatively easy to calculate.

The required microwave reflecting surface is obtained from a succession of such interesting ellipses (as described in Chapter IV) with the proper phase inserted into Equation 23.

B I B L I O G R A P H Y

BIBLIOGRAPHY

1. Silver, S., Microwave Antenna Theory and Design, New York, McGraw-Hill Book Company, Inc., 1949, pp. 158-60.

2. Silver, op. cit., p. 468.

3. Silver, S., Double Curvature Surfaces For Beam Shaping With Point Source Feeds, Massachusetts Institute of Technology Radiation Laboratory Report No. 691, Cambridge, June 15, 1945.

4. Spencer, R. C., Synthesis of Microwave Diffraction Patterns with Application to $\csc^2\theta$ Patterns, Massachusetts Institute of Technology Radiation Laboratory Report No. 272 (54-24), Cambridge, June 23, 1943.

5. Holliman, A. L., Unpublished Notes, Engineering Experiment Station Notebook, Georgia Institute of Technology, 1958.

6. Silver, Microwave Antennas, p. 170.

7. Kraus, J. D., Antennas, New York, McGraw-Hill Book Company, Inc., 1950, pp. 347-8.

8. Silver, Microwave Antennas, pps. 170-4.

9. Hollis, J. S., A Fourier Integral Computer for Calculation of Antenna Radiation Patterns, Unpublished M.S. Thesis, Georgia Institute of Technology, 1956.

10. Hollis, op. cit., p. 5.

11. Kraus, op. cit., p. 343.

12. Hollis, J. S., James, C. E., and Rivers, W. K., Unpublished Notes, Engineering Experiment Station Notebook, Georgia Institute of Technology, 1958.

13. Middlemiss, R. R., Analytic Geometry, New York, McGraw-Hill Book Company, Inc., 1945, p. 191.